

8-12
N80K
TMX —

Reprinted from: CLEAR AIR TURBULENCE AND ITS DETECTION
(Plenum Press, 1969)

LASER BACKSCATTER CORRELATION WITH TURBULENT REGIONS OF THE ATMOSPHERE

N70-70021

J. D. Lawrence, Jr., M. P. McCormick, S. H.
Melfi, and D. P. Woodman*
National Aeronautics and Space Administration

Langley Research Center, Hampton, Virginia

1. INTRODUCTION

A number of light scattering methods have been used to investigate the molecular and particulate content of the atmosphere. They include the searchlight probe studies of Elterman (1954) and Friedland, Katzenstein, and Zatzick (1956), the twilight scattering studies of Volz and Goody (1962) and the aureole photometry of Newkirk and Eddy (1964). With the advent of the high powered ruby laser, optical radar studies of the atmosphere have been made by Fiocco and Smullin (1963), Fiocco and Grams (1964), Clemensha, et al (1965), Bain and Sandford (1966), and Collis and Ligda (1964). Collis (1964) using a ground-based laser radar system observed "ghost" returns from apparently clear air and suggested that they were caused by stratified aerosol layers. It was also suggested that these returns could be used to map effects of air motion and possibly provide an indication of clear air turbulence (CAT). Franken et al (1965) used an airborne system to investigate the correlation between laser returns and clear air turbulence with inconclusive results.

In this paper we describe the results of a series of experiments in which a T-33 type jet aircraft was used to conduct a general search for turbulence in the vicinity of a ground-based laser radar system. In all altitude regions in which the aircraft encountered turbulence in clear air

*College of William and Mary, Williamsburg, Virginia

an enhancement in backscattered laser radiation associated with an aerosol density gradient was observed. These preliminary results indicate that laser radar may be a promising technique for the study of atmospheric turbulence.

2. SCATTERING OF LASER RADIATION IN THE ATMOSPHERE

In order to establish a basis for the interpretation of laser returns from the atmosphere, we shall briefly present in this section a summary of Mie (1908) theory calculations at the ruby laser wavelength for scattering by a clear atmosphere and compare the results obtained with experimental measurements.

The radiation backscattered by a volume element of the atmosphere located at an altitude z from the laser, expressed as the power incident on a coaxial receiver, is given by

$$P(z) = \frac{cE A_R q^2(z) \sigma(z)}{2z^2} \quad (1)$$

where E is the transmitted energy, A_R is the area of the receiver, $q(z)$ is the transmissivity of the atmosphere, $\sigma(z)$ is the backscattering volume cross section of a volume element located at z , and c is the velocity of light. In equation (1) the scattering volume is assumed to be a point source which requires the beam divergence and pulse width of the laser to be small.

The volume cross section and transmissivity will be interpreted according to a scattering model which assumes the atmosphere to be a mixture of molecules, described by Rayleigh (1871) theory, and aerosols, described by rigorous Mie theory.

If atmospheric absorption is neglected the transmissivity is given by

$$q(z) = \exp \left[- \int_0^z \beta(z') dz' \right] \quad (2)$$

where $\beta(z')$ is the sum of the molecular and aerosol scattering coefficients.

2.1 Rayleigh Scattering

The Rayleigh volume cross section for backscatter from the molecular component is

$$\sigma_M = k \bar{\alpha}^2 N(z) f \quad (3)$$

where

k = wave number of incident radiation, $2\pi/\lambda$
 $\bar{\alpha}$ = polarizability
 $N(z)$ = number density
 and

$$f = \frac{3(2 + \Delta)}{6 - 7\Delta}$$

where Δ is the depolarization factor. The polarizability of atmospheric air for optical radiation is $1.73 \times 10^{-24} \text{ cm}^3$, and G. de Vaucouleurs (1951) found f to be 1.054. Equation (3) for incident ruby laser radiation then becomes

$$\sigma_M(z) = 2.11 \times 10^{-23} N_M(z) \text{ km}^{-1} \text{ sterad}^{-1} \quad (4)$$

where $N_M(z)$ is the number of molecules per cubic centimeter. The scattering coefficient for the molecular component is

$$\beta_M(z) = \int_0^{2\pi} \int_0^\pi \frac{1}{2}(1 + \cos^2 \theta) \sigma_M(z) \sin \theta \, d\theta \, d\phi \quad (5)$$

Integration gives

$$\beta_M(z) = 1.77 \times 10^{-22} N_M(z) \text{ km}^{-1} \quad (6)$$

2.2 Large Particle Scattering

The treatment of aerosol scattering given here is similar to a more general treatment given by Bullrich (1964). Assuming that the particulate matter present in the atmosphere may be considered a polydisperse collection of homogeneous spheres of average index η , the volume cross section is given by

$$\sigma_A(z) = \int_{r_1}^{r_2} \frac{i_1(\alpha, \eta, \theta) + i_2(\alpha, \eta, \theta)}{2k^2} dn(r, z) \quad (7)$$

where $i_{1,2}(\alpha, \eta, \theta)$ are the Mie intensity functions for light with electric vector perpendicular and parallel, respectively, to the plane through the direction of propagation of the incident and scattered radiation, r is the radius of the scatterer, $\alpha = 2\pi r/\lambda$ is the particle size parameter, $dn(r, z)$ is the number density of particles with radius between r and $r + dr$ at altitude z , and θ is the scattering angle measured between the direction of the incident and scattered radiation. For atmospheric aerosol distributions which obey the Junge size distribution law, it may be shown that

$$\sigma_A(z) = \frac{v r_1^v N_A(z) \left(\frac{2\pi}{\lambda}\right)^{v-2}}{2 \left[1 - \left(\frac{r_1}{r_2}\right)^v\right]} \int_{\alpha_1}^{\alpha_2} \frac{i_1(\alpha, \eta, \theta) + i_2(\alpha, \eta, \theta)}{\alpha^{v+1}} d\alpha \quad (8)$$

In equation (8), v is the size distribution parameter, $N_A(z)$ is the total aerosol number density and $\alpha = 2\pi r/\lambda$ is the particle size parameter.

Similarly, it may be shown that the aerosol scattering coefficient is given by

$$\beta_A(z) = \frac{v r_1^v N_A(z) \pi \left(\frac{2\pi}{\lambda}\right)^{v-2}}{\left[1 - \left(\frac{r_1}{r_2}\right)^v\right]} \cdot \int_{\alpha_1}^{\alpha_2} \frac{2/\alpha^2 \sum_{m=1}^{\infty} (2m+1) [|a_m(\alpha, \eta)|^2 + |b_m(\alpha, \eta)|^2]}{\alpha^{v-1}} d\alpha \quad (9)$$

where $a_m(\alpha, \eta)$ and $b_m(\alpha, \eta)$ are the Mie coefficients (cf. van de Hulst (1957)).

A computer program has been written to evaluate the integral expressions in equations (8) and (9) for arbitrary choice of aerosol parameters. The recursion relationships of Deirmendjian (1962) were used for calculation of the Mie coefficients which were terminated when the real and imaginary parts of a_m and b_m were all less than 10^{-8} .

For computational purposes, an average index of refraction $\eta = 1.5$ has been assumed. This value is consistent with the composition of aerosol particles collected by Junge et al (1961) and is in agreement with the conclusions reached by Bullrich (1964) in his review of composition data.

Junge (1963) suggests a value $\nu = 3$ for large aerosol concentrations near the ground which is also consistent with the optical measurements of Bullrich (1964) and Volz (1956). Evaluation of equations (8) and (9) also requires a choice of particle radii limits. We have adopted a particle size range of $0.1\mu \leq r \leq 20\mu$ in order to derive an aerosol volume cross section and scattering coefficient consistent with direct sampling measurements.

For $\eta = 1.5$, $\theta = 180^\circ$, $\nu = 3.0$, $\lambda = 6943 \text{ \AA}$, $r_1 = 0.1\mu$, $r_2 = 20\mu$, equations (8) and (9) give for the volume cross section and scattering coefficient

$$\sigma_A(z) = 0.577 \times 10^{-5} N_A(z) \text{ km}^{-1} \text{ sterad}^{-1} \quad (10)$$

and

$$\beta_A(z) = 1.54 \times 10^{-4} N_A(z) \text{ km}^{-1} \quad (11)$$

A comparison of the vertical profile calculated on the basis of this scattering model and one measured by a ruby laser radar system is given in Figure 1. In Figure 1 the dotted line is the vertical profile for the molecular component calculated from equations (4) and (6) using the number density profile of the U.S. Standard Atmosphere 1962. Shown as a solid line is the total calculated vertical profile. The aerosol component of this curve was computed from equations (10) and (11) for Rosen's (1966) measured aerosol number density profile. Shown also in Figure 1 are

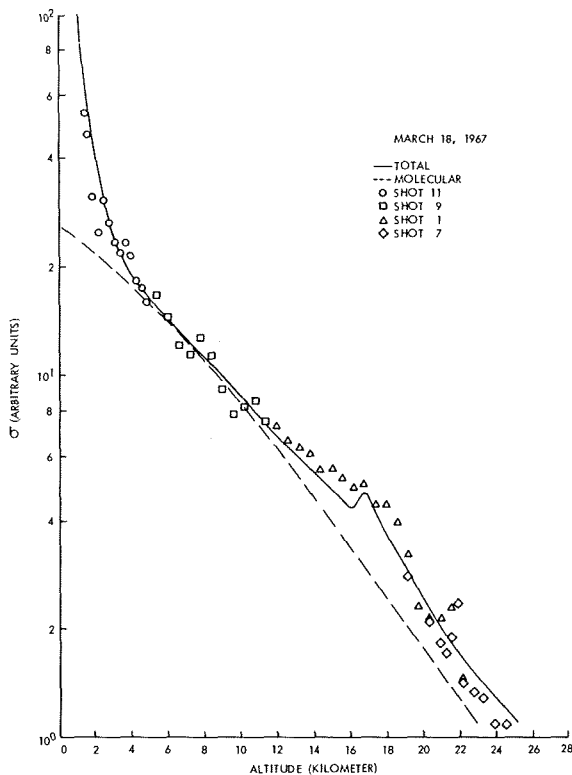


Figure 1. Backscatter volume cross section (σ) as a function of altitude for March 18, 1967.

sections of four laser soundings which have been normalized to the molecular scattering model at 9 km. The model calculation generally agrees very well with the experimental data and, in consequence, provides a basis for interpreting laser backscatter measurements in terms of the spatial density of molecules and aerosols.

We would also like to note that although the general agreement between the experimental data and the model calculation is good, significant deviations over relatively small altitude regions do occur in the clear atmosphere. For example, in Figure 1 significant deviations from the normal clear air profile are evident from 7-9 km and also

in the vicinity of 21 km.

On the basis of the scattering model discussed in the preceding paragraphs, we believe that such deviations from the clear air profile of the magnitude observed must be produced by local aerosol concentrations possibly coupled with variations in the size distribution or index of refraction. In a section to follow we describe the correlation established between regions of enhanced laser backscatter as discussed above and atmospheric turbulence.

3. DESCRIPTION OF LASER RADAR EQUIPMENT

3.1 General

A schematic diagram of the laser radar equipment used to make the measurements described in this paper is given in Figure 2. The system consists of a ruby laser and 1.52

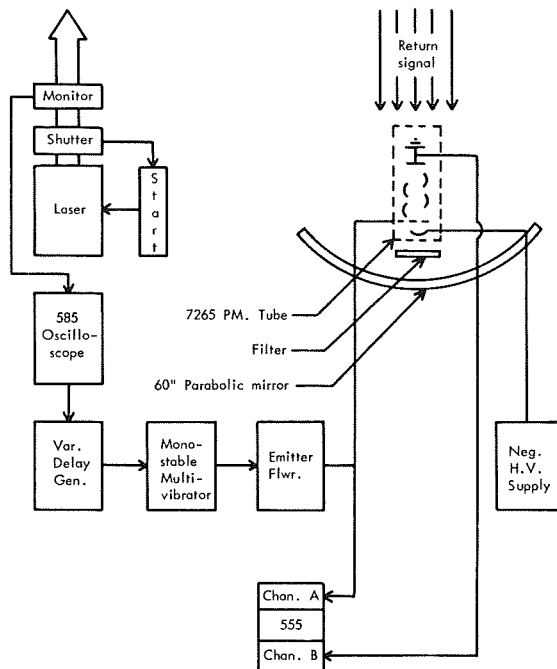


Figure 2. A block diagram of the experimental arrangement.

meter parabolic searchlight mirror positioned in a steerable mount with their axes aligned parallel. The laser pulse is monitored with a set of beam splitters whose axes are separated by 90° allowing a portion of the beam to fall on a diffuse white screen which lies in the field of view of a photodiode. The beam splitters' orientation provides polarization insensitivity. The output of the photodiode is displayed on an oscilloscope and provides a measure of the laser pulse width. The charge through the photodiode gives a number proportional to the total number of emitted photons and the total light energy. This charge is stored in a capacitor and the resulting voltage is measured by an electrometer giving an energy measurement to within $\pm 10\%$. After passing through the energy monitor the laser pulse passes through a rotating shutter which prevents fluorescence radiation from leaving the laser system. The rotating shutter is a balanced aluminum disk which is rotated by a 400 cycle hysteresis synchronous motor at 13,500 rpm. A magnetic pickup device is positioned near the disk and provides a pulse to trigger the laser. This pulse is delayed so that the shutter opening is aligned with the laser exit port at the time when the laser Q-switches.

Before the laser is fired the focus electrode of the photomultiplier detector is biased 30 v negative with respect to the cathode, thereby defocusing the tube. A monostable multivibrator is triggered by a delayed pulse derived synchronous with the emission of the giant laser pulse. The monostable multivibrator produces a positive gate with a rise time of about 1 μ sec and a variable width and height. This gate is applied to the focusing electrode, thereby focusing the detector for a length of time determined by the gate width. The anode of the photomultiplier is directly coupled to a variable gain operational amplifier used to limit the frequency passband of the system.

3.2 Receiver System

The receiver system consists of a 1.52 meter searchlight mirror (focal length = 25.54 inches) in a steerable mount. The photomultiplier detector is positioned behind the focal plane on a precision mount with five degrees of freedom. An iris is used to limit the field of view of the mirror to a calculated value of about 10 milliradians. In order to limit the night-sky background, a Wratten No. 70

filter is positioned in front of the photomultiplier. This filter has a sharp cutoff at 6500 Å and, when used in conjunction with a photomultiplier having an S-20 photocathode spectral response, gives a bandpass of about 700 Å.

3.3 Laser System

The laser system contains a 7 x ½" Brewster angle ruby rod which is Q-switched by uranyl glass. The system has a maximum energy output of approximately 2 joules with a pulse width of 30 nsec. The full width beam divergence is approximately 6 mrad and in view of the relatively large field of view of the receiver further collimation of the beam is not necessary. The entire laser system is enclosed in a light-tight container and is temperature controlled to prevent detuning into a water vapor absorption band.

3.4 System Performance

In view of the wide spectral bandwidth of the system, it can not of course be used to make measurements during the daylight hours. At night, however, the sky background radiance is down from its daylight value by approximately six orders of magnitude and its contribution to the system noise is negligible for altitudes below approximately 30 km. As an indication of the performance of the system during nighttime operation we have listed in Table 1 values of the signal to noise ratio for several altitude regions:

TABLE 1. SYSTEM DETECTION CAPABILITY

Altitude (km)	Signal to noise ratio
5	200
10	76
15	37
20	20
26	10

4. EXPERIMENTAL RESULTS AND DISCUSSION

In a series of experiments performed over Williamsburg and Wallops Island, Virginia, a T-33 type jet aircraft equipped with a recording accelerometer was used to conduct a general search for turbulence in the vicinity of the laser radar system. During the coordinated experiment the aircraft flew in an elliptical path downwind of the field station as shown schematically in Figure 3.

As the aircraft ascended, a number of laser radar soundings of the atmosphere were made with the gain and range gate of the system set to observe an altitude region corresponding to the position of the aircraft. After the aircraft attained its maximum altitude in the vicinity of 12.2 km, the pilot was asked to descend and probe altitude regions where the laser radar sounding showed an enhancement or a sharp discontinuity. On the basis of the pilot report, verified by the recording accelerometer, the altitude regions of the atmosphere which were turbulent at the time of a laser sounding were established. In addition in all altitude regions which showed enhancement backscattering,

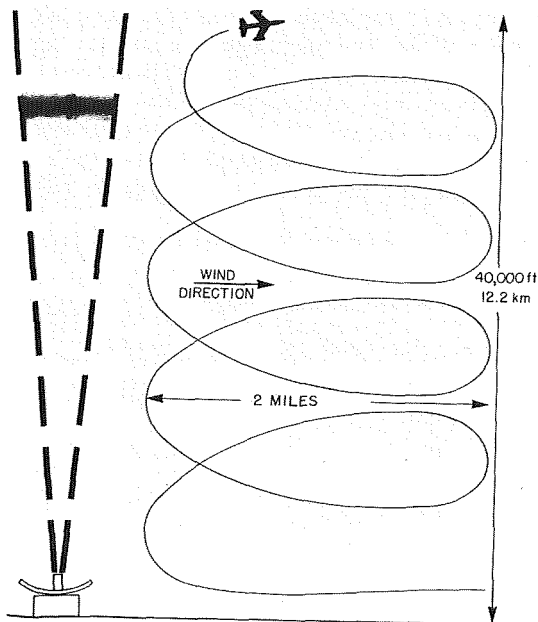


Figure 3. The geometry of the CAT experiment.

the pilot was asked to look for haze and in three of the experiments, he was assisted by a searchlight.

In all altitude regions in which the aircraft encountered turbulence in clear air an enhancement or sharp discontinuity in the laser backscattering profile associated with an aerosol density gradient was observed. Figure 4 shows three typical oscilloscope recordings of the laser return from altitude regions in which the aircraft encountered light turbulence. An enhancement is evident in Figure 4(a) from 3.3 to 4.1 km; the pilot reported light turbulence (0.1 to 0.2 g) in clear air from 3.7 to 4.1 km. In Figure 4(b) an enhancement extending from 2.4 to 3.1 km is evident; the pilot reported light turbulence (0.1 to 0.2 g) in clear air in three layered regions extending from 2.5 to 2.8 km. Radiosonde measurements made 75 miles away from the site of the experiment on this evening indicated that a subsidence

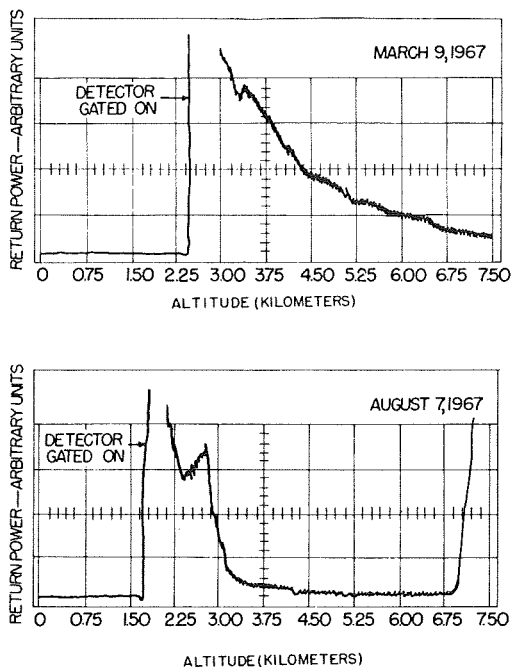


Figure 4a, 4b. Oscilloscope recording of return power as a function of altitude for March 9 and August 7, 1967, respectively.

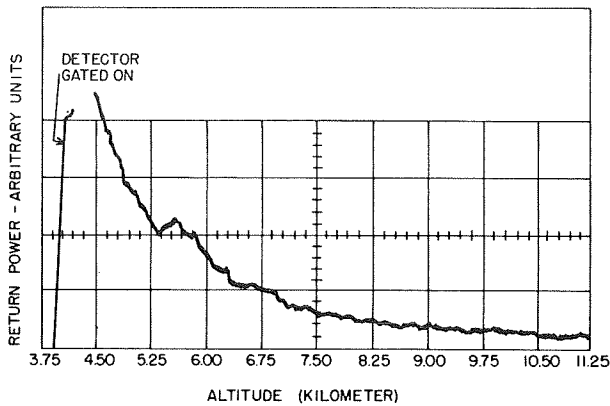


Figure 4c. Oscilloscope recording of return power as a function of altitude for April 11, 1968.

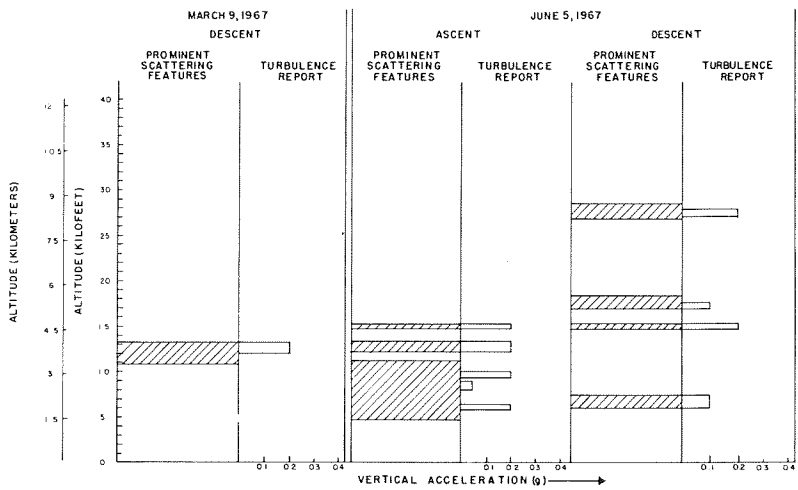


Figure 5a. Prominent laser radar scattering features and aircraft accelerometer recordings versus altitude for March 9 and June 5, 1967.

inversion existed at an altitude of 3.1 km; light turbulence was present beneath this inversion. In Figure 4(c) an enhancement is evident at 5.3 km; the pilot reported light turbulence in a thin stratified region at 5.3 km. This scattering feature did not correlate with any of the physical parameters measured by a balloon sounding made at approximately the same time and was not present during the ascent of the aircraft.

Figure 5 presents a summary of the results obtained during four nights of observation and are typical of the results obtained during the other three nights of observation. The results presented in Figure 5(c) for the night of March 14, 1968, require further explanation. On this particular evening an enhancement in the backscattered radiation was evident in the vicinity of 3.4 km which was not turbulent; radiosonde measurements indicated that this feature was a relatively thin moisture layer, and clouds were reported at that altitude approximately 4 hours later. In addition, during the ascent of the aircraft, very light turbulence was reported at approximately 6.5 km. The laser

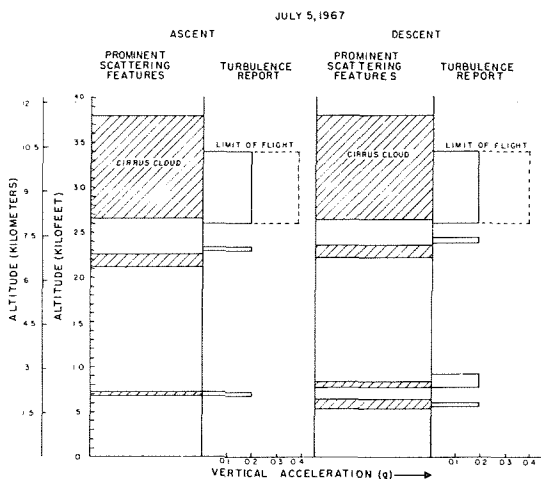


Figure 5b. Prominent laser radar scattering features and aircraft accelerometer recording versus altitude for July 5, 1967. The dotted lines represent regions in which accelerations of 0.4 g were occasionally recorded.

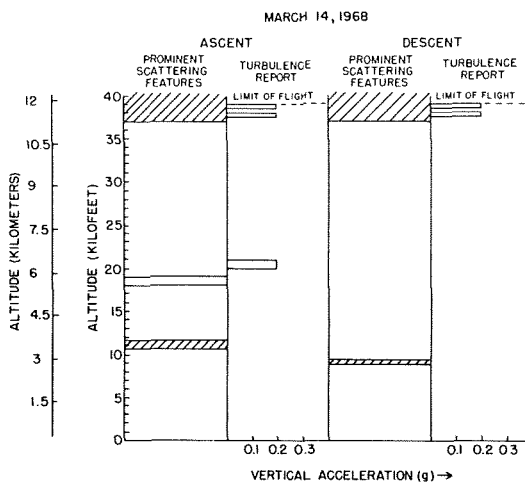


Figure 5c. Prominent laser radar scattering features and aircraft accelerometer recordings versus altitude for March 14, 1968.

radar sounding of this altitude region was delayed approximately 10 minutes by equipment adjustments, and at the time the sounding was made a very weak scattering feature was present at about 5.3 km. This altitude region was carefully probed approximately 45 minutes later during the descent of the aircraft and was not turbulent, nor did it exhibit any unusual scattering features. The scattering feature evident in Figure 5(c) with its base at 11.5 km corresponds to the tropopause for this particular evening; the aircraft reported light turbulence in two layered regions from the base of this scattering feature to the altitude limit of the aircraft.

To summarize the results obtained to date, a total of 33 cases of correlation of turbulence as experienced by the aircraft and prominent scattering features as measured by a laser radar system have been found. In addition, in all altitude regions in which the aircraft encountered turbulence, with the possible exception of the case discussed in the preceding paragraph, an enhancement in back-scattered radiation associated with an aerosol density gradient was observed.

In view of the promising preliminary results obtained in this series of experiments, a future program is planned to extend laser backscatter observations of atmospheric turbulence to higher altitudes and to make observations of mountain-wave turbulence. In conjunction with these observations, comprehensive meteorological measurements will be made in order to evaluate the physical parameters which may be of significance in the determination of the laser radar cross section associated with regions of atmospheric turbulence.

REFERENCES

1. Bain, W. C. and Sandford, M. C. W. (1966). Light scatter from a laser beam at heights above 40 km. J.A.T.P. 28, 543.
2. Bullrich, K. (1964). Scattered radiation in the atmosphere and the natural aerosol. Advances in Geophysics No. 10. (Academic Press, New York), 99.
3. Clemensha, B. R., Kent, G. S., and Wright, R. W. H. (1965). A study of the feasibility of measuring atmospheric densities by using a laser-searchlight technique. AF-AFOSR, 616.
4. Collis, R. T. H., Fernald, F. G., Ligda, M. G. H. (1964). Laser radar echoes from a stratified clear atmosphere. Nature 203, 1274.
5. Collis, R. T. H., and Ligda, M. G. H. (1964). Laser radar echoes from the stratified clear atmosphere. Nature 203, 503.
6. de Vaucouleurs, G. (1951). Constantes de la diffusion Rayleigh dans les gaz et les liquides. Ann. Phys. 6, 211.
7. Deirmendjian, D., and Clasen, R. J. (1962). Light scattering on partially absorbing homogeneous spheres of finite size. U.S.A.F. Project Rand, R-393-PR.
8. Elterman, L. (1954). Seasonal trends of temperature, density, and pressure in the stratosphere obtained with

- the searchlight probing technique. J. Geophys. Res. 59, 351.
9. Fiocco, G. and Grams, G. (1964). Observations of the aerosol layer at 20 km by optical radar. J. A. S. 21, 323.
 10. Riocco, G. and Smullin, L. D. (1963). Detection of scattering layers in the upper atmosphere (60-140 km) by optical radar. Nature 199, 1275.
 11. Franken, P. A., Jenney, J. A., and Rank, D. M. (1965). Airborne investigation of clear air turbulence with optical radar. Progress Report, University of Michigan.
 12. Friedland, S., Katzenstein, J., and Zatzick, M. (1956). Pulsed searchlighting the atmosphere. J. Geophys. Res. 61, 415.
 13. Junge, C. E. (1963). Air Chemistry and Radioactivity. (Academic Press, New York).
 14. Junge, C. E., Manson, J. E. (1961). Stratospheric aerosol studies. J. of Geophys. Res., 66, 2163.
 15. Mie, G. (1908). Beitrage zur Optik trüber Medien, speziell kolloidaler Matallösungen. Ann. Physik 25, 377.
 16. Newkirk, G. Jr., Eddy, John A. (1964). Light scattering by particles in the upper atmosphere. J. of the Atmos. Sci. 21, 35.
 17. Rayleigh, J. W. S. (1871). The theory of sound. Phil. Mag., 41, 107, 274, 447.
 18. Rosen, J. M. (1966). Correlation of dust and ozone in the stratosphere. Nature 209, 1342.
 19. U. S. Standard Atmosphere, (1962). U. S. Government Printing Office, Washington, D. C., December.
 20. van de Hulst, H. C. (1957). Light Scattering by Small Particles. (John Wiley and Sons, Inc.).

21. Volz, F. (1956). Optik der Tropfen. Hanbuch der Geophysik VIII 14, 822.
22. Volz, F. E., and Goody, R. M. (1962). The intensity of the twilight and upper atmospheric dust. J. of the Atmos. Sci. 19, 385.

DISCUSSION

Douglas K. Lilly: I think the light turbulence in the reflective region is probably produced by convection associated with radiative cooling at the top of the layers.

Samuel Harvey Melfi: Thank you for your comment concerning the mechanism of the light turbulence the aircraft experienced. We do not fully understand the mechanism that would produce this correlation, but we will be studying this aspect in the future.